SMiRT-12 / K. Kussmaul (Editor)

L02/1

AN EXPERIMENTAL ANALYSIS OF THE THERMOMECHANICAL BEHAVIOUR OF A Cu-Zn-Al SHAPE MEMORY ALLOY

A. Chrysochoos, H. Pham and O. Maisonneuve

Laboratoire de Mécanique et Génie-Civil, URA CNRS 1214, Université Montpellier II, c.c. 081, place Eugène Bataillon, F-34095 Montpellier Cedex 5, France

Abstract: Using infrared technics, the thermomechanical behaviour of a Cu-Zn-Al alloy is observed during mechanical solicitations at constant room temperature. The phase transition appears to be a non isothermal and non dissipative process. The incidence of this statement is tested on classical modelling approaches through numerical simulations.

1 INTRODUCTION

Several authors [Frémond, 1987; Lexcellent, 1991; Patoor, 1987], use the possible occurrence of dissipative phenomena accompanying the martensitic phase transformation to describe the hysteresis of "pseudo-elastic" behaviour of shape memory alloys.

On the other, Van Humbeek et al. (1987) show that the temperature variations of the material, due to the martensitic transition, could explain the existence of the hysteresis loop.

The hysteresis area exhibits an amount of mechanical energy that can be interpreted as an internal energy variation for the material. Nowadays, the literature does not provide with any clue to conclude wether this variation is converted into dissipated energy, stored energy or latent heat.

After a brief presentation of the theoretical interpretation framework, an experimental analysis of the "pseudo-elastic" behaviour of shape memory alloys will be put forward. From thermal data given by an infrared device, non negligible temperature variations have been recorded in the case of load-unload cycles at constant room temperature. These observed variations are so that no heat is globally exchanged between the sample and the surroundings, at the end of each hysteresis loop. Then, associating a thermodynamic cycle to each loop yields an intrinsic dissipation identically equal to zero. In a last part, numerical simulations of the hysteresis phenomena are performed using classical modelling approaches. The predicted mechanical responses are compared, assuming first an isothermal and dissipative process, and second, a non-isothermal and non-dissipative process.

2 THERMODYNAMIC FRAMEWORK

Classical concepts and results of the Thermodynamics of Irreversible Processes are used, [Boccara, 1968; Germain, 1973]. The thermodynamic state of a volume element is characterized at each instant t, by a set of n + 1 state variables. Let us take T ($T = \alpha_0$) the absolute temperature, ε the strain tensor ($\varepsilon = \alpha_1$) and α_i, i = 2,..., n, a set of n - 1 internal

variables completing the description of the thermodynamic state. The specific Helmholtz free energy is denoted by ψ and s symbolizes the specific entropy.

As a function of the chosen variables, the local form of the second principle leads to the inequality of Clausius-Duhem:

$$D = \sigma : \dot{\varepsilon} - \rho \frac{\partial \psi}{\partial \alpha_j} \dot{\alpha}_j - \frac{\vec{q}}{T} \overrightarrow{\text{grad}T} \geq 0 \, , \; j = 1,..., n, \tag{1}$$

where σ is the Cauchy stress tensor, ρ the mass density, $\vec{q}$ the heat influx vector, and D the dissipation. When D is equal to zero, the irreversible entropy supply D/T is equal to zero, the processes are then reversible. Classically, the intrinsic dissipation is supposed to be positive and is written as:

$$D_1 = \sigma : \dot{\varepsilon} - \rho \frac{\partial \psi}{\partial \alpha_j} \dot{\alpha}_j \geq 0 \, , \; j = 1,...,n. \tag{2}$$

In the experimental conditions of the tests presented here, it is shown in [Chrysochoos, 1992], that the heat conduction equation can be simplified as:

$$\rho C_\alpha \dot{\theta} - k\Delta\theta = D_1 + \rho T \frac{\partial^2 \psi}{\partial T \partial \alpha_j} \dot{\alpha}_j = w'_{ch} \, , \; j = 1,..., n, \tag{3}$$

where $\theta = T - T_0$, with T_0 the equilibrium temperature field. The specific heat C_α and the isotropic conduction tensor k are supposed to be constant. In the second member of equation (3), the intrinsic dissipation and the crossing terms corresponding to the thermomechanical couplings, are gathered. The term w'_{ch} symbolizes the volume heat sources.

3. EXPERIMENTAL ANALYSIS

3.1 Experimental arrangement

The experimental set-up is essentially made of a testing machine and an infrared camera [Chrysochoos, 1992].

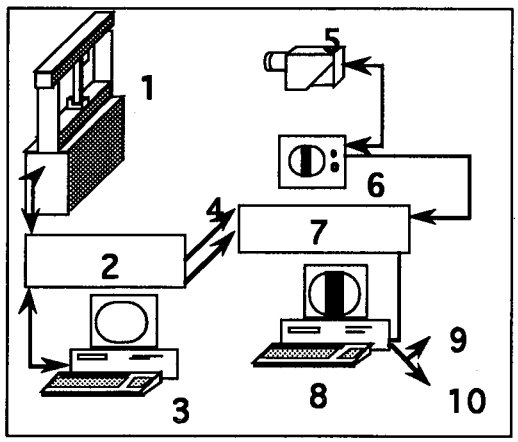

Fig. 1: Basic sketch of the set-up
1: uniaxial testing machine (100 kN). **2**: command unit. **3**: micro-computer #1: loading parameters control, mechanical data storage and processing. **4**: transfer unit for load, stroke and extensometer signals. **5**: infrared camera; Insb detector, liquid nitrogen cooled. **6**: display unit. **7**: numerization system of the video signal (THERMAK). **8**: micro-computer #2: storage, visualization, and processing of the thermal data. **9**, **10**: printer or plotter output.

Mechanical tests are performed with a computerized uniaxial testing machine (**1, 2, 3**). The infrared thermography device is made of the camera (**5**), the display unit (**6**) and the numerization system (**7**) allowing the storage of thermal pictures in a second microcomputer (**8**). The pictures are matrixes of 256 lines per 180 columns numerized on 12 bits.

The numerization system allows to record, by the means of (**4**), the load and deformation signals.

3.2 Linking the temperature field to the heat source

The calibration of the video signal is performed using a special warming target equipped with thermocouples. The calibration law is strongly non linear even near thermal equilibrium. It has been approximated by a quadratic law (second order approximation).

The temperature variations are obtained relatively to a reference thermal picture. The evaluation of w'_{ch} volume amount is deduced from a numerical estimation of the time derivative and the laplacian of the temperature.

In the particular case of quasi-static and homogeneous tests, a linearization of the thermal losses is possible. Then, the local equation of heat conduction becomes:

$$\rho C_\alpha \left(\frac{\partial \theta}{\partial t} + \frac{\theta}{\tau_{th}}\right) = w'_{ch} \quad , \tag{4}$$

where τ_{th} is a constant characterizing the thermal losses. The energy amounts are calculated for the gauge volume V_0 of the sample ($V_0 = 150$ mm^3):

$$W_{ch}(t) = V_0 \int_0^t w'_{ch}(\tau)\, d\tau \, . \tag{5}$$

3.3 Experimental results

3.3.1 Sample and experiment

Flat samples of Cu-70.17% Zn-25.63% Al polycrystalline alloys have been used. The transformation temperatures of such an alloy are the following: $M_S = 15$ °C, $M_f = 6$ °C, $A_S = 7$ °C, $A_f = 19.5$ °C. The slope of the transition line is around 2 MPa °C^{-1}.

The thermoelastic constants of the material are: $E = 24$ GPa (Young's modulus), $\nu = 0.33$ (Poisson's ratio), $\lambda_{th} = 18.10^{-6}$ °C^{-1} (thermal expansion), $\rho = 7700$ kg m^{-3} (mass density), $C = 393$ J kg^{-1} °C^{-1} (specific heat) et $k = 80$ W m^{-1} °C^{-1} (thermal conductivity). The room temperature is constant and is equal to 30 °C.

To insure an initial austenitic state, the samples are annealed at 850 °C during 10 mn and then oil-quenched [Vacher, 1991] during one hour [Vacher, 1991]. The storage temperature of samples is greater than 35 °C. Just before testing, a thin coat of black painting is laid down on the surface of the samples to improve its emissivity.

Two kinds of experiment have been performed: load-unload paths with increasing amplitude of strain ($\varepsilon_{max} = 0.5\%, 1\%, 1.5\%$) and load-unload paths with constant amplitude ($\varepsilon_{max} = 1\%$). The solicitations are strain controlled during the loading and stress controlled during the unloading to avoid buckling phenomena.

The figures 1 and 2 give the evolutions of the deformation. The absolute value of the strain rate is less than 1.10^{-3} s^{-1}. The corresponding hysteresis loops can be observed on figures 3 and 4. Finally, the evolution of θ and W_{ch} are plotted on figures 1 and 2.

3.3.2 Observations

Observation 1: The amplitude of temperature variations is around 3°C. These variations are small compared to absolute temperature but they are not negligible in comparison with the size of the transition domain (A_f - $M_f \approx$ 13.5 °C).
Observation 2: The amount of heat W_{ch} exchanged between the sample and the surroundings returns to zero at the end of each hysteresis loop.

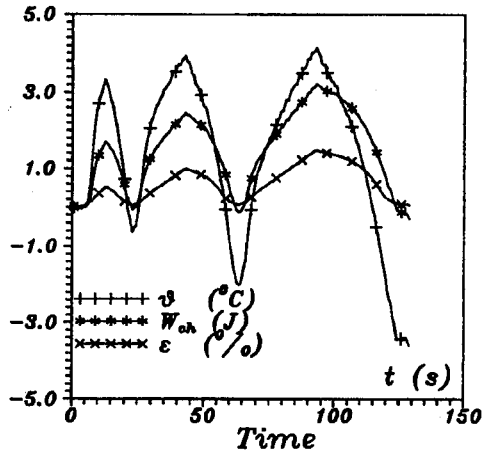

Fig.1: Load-unload cycles with increasing amplitude. Thermal response and evolution of heat (deduced from the thermal data). This energy amount returns to zero at the end of each cycle.

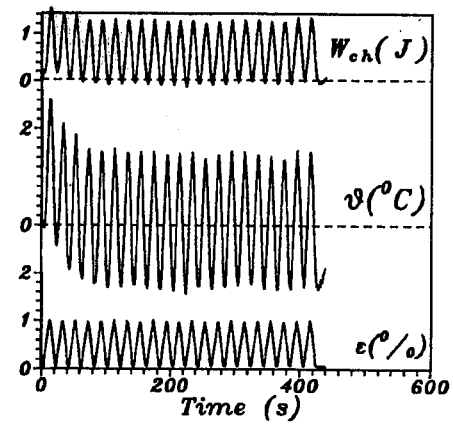

Fig.2: Load-unload cycles with constant amplitude. Thermal response becomes periodic and symmetric after few cycles. The heat W_{ch} returns to zero at the end of each hysteresis loop.

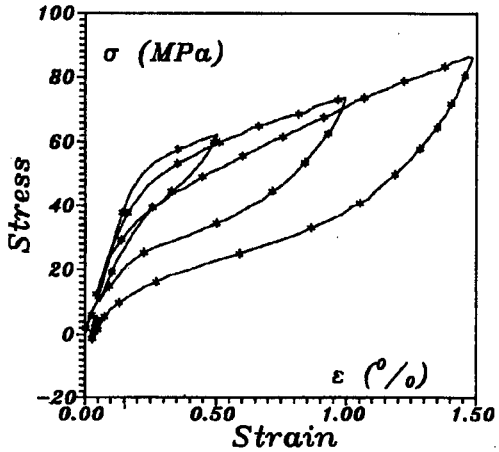

Fig. 3: Mechanical response. Hysteresis loops increasing.

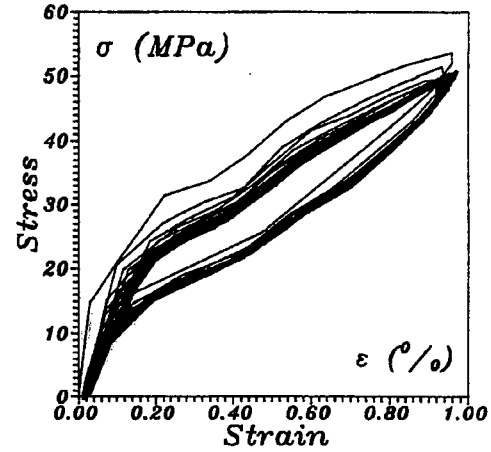

Fig.4: Mechanical response. Stabilization of hysteresis loops.

3.3.3 Discussion

Consequently, rather than assuming an isothermal process ($T = T_0$), a linearized thermal approach ($\theta / T_0 << 1$) will be tested in part 4.

Now, let us precise first, the conditions required to associate a thermodynamic cycle with each hysteresis loop, so that we get:

$$\int_C W'_{ch}(\tau)\, d\tau = 0, \tag{6}$$

where C is the duration of the cycle. And second, let us show that the intrinsic dissipation D_1 remains identically equal to zero during such a thermodynamic cycle.

At the end of each hysteresis loop, the deformation comes back to its initial value within about the thermoelastic strain that is hardly measurable. Moreover, the internal state of the material is afresh austenitic as soon as the stress is equal to zero for a temperature greater than A_f. We shall suppose, *a priori* , that the internal state variables (α_i), i = 2,..., n, take their initial values again. The temperatures observed at the beginning and at the end of the loop can be naturally different, because of the heat diffusion. Both following cases occur:

i) the temperatures T_i and T_f are the same, (see the case of constant amplitude pulsating tests, after several load-unload cycles (fig.2)). In such a case, each loop represents a thermodynamic cycle.

ii) the temperature T_i and T_f are different, but they remain greater than A_f. Then the thermodynamic cycle can be closed using two thermoelastic transformations, the stress being equal to zero. These fictitious transformations assure respectively the passage from T_0 to T_i, and from T_f to T_0. Assuming a linear and isotropic thermoelastic behaviour, the amount of heat evolved by both transformations can be written as:

$$[W_{ch}]_0^i + [W_{ch}]_f^0 \approx -V_0\left[\lambda_{th}^2\, T_0\, E\, (T_i - T_f)\right]. \tag{7}$$

For a maximal spread corresponding to 2 Celsius degrees between T_i and T_f, the value of the energy defined by (7) is around 2.10^{-3} J and corresponds to a strain amplitude less than 10^{-4}. These orders of magnitude are so small that they cannot be detected by our captors.

Then, associating a thermodynamic cycle to each hysteresis loop, that verifies the equation (6), seems to agree with our observations. Now, let us show that the dissipation is identically equal to zero during such a cycle, if the temperature variations remain small.

For all thermodynamic cycle of duration C, we then have:

$$\int_C \rho\, \dot{s}\, dt = \int_C \rho\, C_\alpha \frac{\dot{T}}{T} dt - \int_C \rho \frac{\partial^2 \psi}{\partial \alpha_j \partial T} \dot{\alpha}_j\, dt = 0, \text{ for } j = 1,..., n. \tag{8}$$

The first integral in the right hand of (8), being equal to zero, the second one is also equal to zero. Then taking into account the small variations of θ ($\theta/T_0 < 2\%$), a linearized version of (3), integrated on the cycle yields $D_1 \equiv 0$.

This result is established for a polycrystalline alloy, in the case of mechanical solicitations at constant room temperature. It can be compared with the one obtained by differential

calorimetry on the same alloy, during thermal solicitations when the stress is equal to zero [Ortin, 1988].

In every case, it appears that if the intrinsic dissipation takes place, it remains very small in comparison with the latent heat rate of phase change.

Table 1 describes, in the case of cycles with increasing deformation amplitude, the relative importance of dissipated energy against thermomechanical couplings' energies. On the one hand, this importance can be traduced by the ratio R_T defined in (9-a). This ratio is equal to 1, when the behaviour is exclusively dissipative (without thermomechanical couplings), and it is equal to zero when the behaviour is non dissipative. On the other hand, the hysteresis area can be characterized from a mechanical viewpoint, by the ratio R_M defined by (9-b).

(9-a) $$R_T = \frac{\int_C w'_{ch}(t)\,dt}{\int_C |w'_{ch}(t)|\,dt},$$ (9-b) $$R_M = \frac{\int_C \sigma\dot{\varepsilon}\,dt}{\int_{Load} \sigma\dot{\varepsilon}\,dt}.$$

The integral $\int_C \sigma\dot{\varepsilon}\,dt$ represents the volume energy associated with the hysteresis area.

Tab. 1: Evolution of the ratios R_T and R_M during the tests with increasing amplitude of deformation.

ε_{max} (%)	$V_0\int_C \lvert w'_{ch}\rvert\,dt$ (10^{-3} J)	R_T (%)	$V_0\int_C \sigma\dot{\varepsilon}\,dt$ (10^{-3} J)	R_M (%)
0,5	3585	2,1	6	18
1,0	5173	2,7	27	34
1,5	8010	0,5	55	43

First, note that the ratio R_T remains very small, which is in good agreement with a non-dissipative phase transformation hypothesis. Second, one can observe very weak amounts of mechanical energy corresponding to the hysteresis area (less than 1.10^{-2} J) in comparison with the latent heats (greater than 1. J). Third, the "hysteresis energy" is not negligible against the mechanical energy provided by the testing machine to deform the sample ($R_M > 15$ %).

4 CONSEQENCE OF THE EXPERIMENTAL RESULTS ON CLASSICAL MODELS

In this part the numerical predictions of two classical modellings are compared, assuming either an isothermal and dissipative phase transition (hypothesis H_1) or a non-isothermal and non-dissipative phase transition (hypothesis H_2).

Both models belong to the formalism of the Generalized Standard Materials [Halphen, 1975]. The thermomechanical behaviour of the material is then described by two potentials: a thermodynamic potential and a pseudo-potential of dissipation. In most cases, the specific Helmholtz free energy ψ is chosen. The dissipation potential is taken as a positive convex function of the state variables rate $\dot{\alpha}_i$, and it is equal to zero at the origin. These properties insure the validity of Clausius-Duhem inequality.

The state variables are T, ε, β, where $\beta = (\beta_1,..., \beta_m)$ is the volume proportions of the m martensite twins. The mass balance implies the following inequalities:

$$(10) \qquad 0 \le \beta_l \le 1\ ,\ l = 1,..., m\ ;\ \text{and}\ 0 \le \sum_{l=1}^{m} \beta_l \le 1.$$

The mathematical treatment of (10) uses the basic convex analysis tools. The term $\partial f(x_0)$ denotes the subdifferential in x_0 of the convex function f defined on $\mathbb{R}^n$. It is reminded that:

$$(11) \qquad \partial f(x_0) = \{y \in \mathbb{R}^n / f(x) \ge f(x_0) + (x - x_0).y,\ \forall x \in \mathbb{R}^n\}.$$

If f is a regular function in x_0 then $\partial f(x_0)$ is reduced to the gradient of f in x_0.

4.1 Model 1 based on a Frémond's approach

The following expression of the specific free energy is adopted for the particular case in which two martensite twins are taken into account [Frémond, 1987]:

$$(12) \qquad \rho\,\psi(T,\varepsilon,\beta) = \rho\,(1 - \beta_1 - \beta_2)\,\psi_a(T,\varepsilon) + \rho \sum_{l=1}^{2} \beta_l\,\psi_{ml}(T,\varepsilon) + I(\beta),$$

The mass density ρ is supposed to be the same for all phases; the terms ψ_a, ψ_{m1}, ψ_{m2} are respectively the specific free energy of the austenite phase, and the specific free energies of the martensite twins. Phase interactions are not taken into account. The symbol I (β) represents the indicator function of the following convex set $\mathcal{C}$:

$$\mathcal{C} = \{(\gamma_1,\gamma_2) / 0 \le \gamma_k \le 1,\ k = 1, 2 \text{ and } 0 \le \gamma_1 + \gamma_2 \le 1\}$$
$$I(\beta) = 0 \text{ if } \beta \in \mathcal{C} \text{ and } I(\beta) = +\infty \text{ if } \beta \notin \mathcal{C}\ .$$

If the dissipation is exclusively due to the phase change, the dissipation potential solely depends on the rate of β. The state laws are:

$$(13) \qquad \sigma = \rho\,(1 - \beta_1 - \beta_2)\frac{\partial \psi_a}{\partial \varepsilon}(T,\varepsilon) + \rho \sum_{l=1}^{2} \beta_l \frac{\partial \psi_{ml}}{\partial \varepsilon}(T,\varepsilon)\ ;$$

$$(14) \qquad B_l = \rho\,(\psi_{ml}(T,\varepsilon) - \psi_a(T,\varepsilon))\ ,\ \text{for } l = 1, 2;$$

$$(15) \qquad -B \in \partial I(\beta) + \partial \phi(\dot{\beta})\ ,\ \text{with } B = (B_1,B_2).$$

In the case of a non-dissipative behaviour, the state law (15) becomes:

$$(16) \qquad -B \in \partial I(\beta)\ ,\ \text{with } B = (B_1,B_2).$$

In such a case, the "pseudo-elastic" hysteresis cannot be obtained under isothermal testing hypothesis [Frémond, 1987]. At least, Frémond suggested to transform the triangle defined by $\mathcal{C}$ in a curvilinear triangle included in $\mathcal{C}$ to take into account phase interactions. Other trials

can be seen in the literature (see for example [Müller et al., 1991]). The following model try to consider these interactions through an "interaction specific energy".

4.2 Model 2 based on a Lexcellent-Licht's approach

In this model [Lexcellent, 1991], the expression of the free energy is deduced from the specific enthalpy defined by [Patoor, 1987], using the Legendre-Fenchel transform. An indicator function $I(\beta)$ is introduced in the free energy form to improve the formal coherence of the model:

$$(17)\quad \rho\,\psi(T,\varepsilon,\beta) = W_{elast}\left(\varepsilon - g\sum_{l=1}^{m} R_l\beta_l\right) + \left(\sum_{l=1}^{2}\beta_l\right) W_{chem}(T) + W_{int}(\beta) + I(\beta).$$

The terms W_{elast}, W_{chem}, W_{int} symbolize respectively the elastic energy, the chemical energy and the energy of interactions. The sum $g\sum R_l\beta_l$ represents the deformation due to phase changes. If dissipation potential ϕ solely depends on the rate of β, then the state laws are:

$$(18)\quad \sigma = \frac{\partial W_{elast}}{\partial \varepsilon}\left(\varepsilon - g\sum_{l=1}^{m} R_l\beta_l\right);$$

$$(19)\quad B_l = -gR_l\sigma + W_{chem}(T) + \frac{\partial W_{int}}{\partial \beta_l}(\beta),\ l = 1,\ldots, m;$$

$$(20)\quad -B \in \partial I(\beta) + \partial\phi(\dot{\beta}),\ \text{with } B = (B_1,\ldots, B_m).$$

In the case of a non dissipative behaviour, the state law (20) becomes:

$$(21)\quad -B \in \partial I(\beta),\ \text{with } B = (B_1,\ldots, B_m).$$

As in the former model, the state laws cannot predict the pseudo-elastic hysteresis if the temperature is constant. In such a case, the equations (19) and (21) define a map-to-map relationship between σ and β (W_{int} being supposed strictly convex).

4.3 Numerical results

One-dimensional numerical simulations are performed. Load-unload cycles are considered and it is supposed that only one martensite twin is activated. The room temperature is constant and greater than A_f. For both models a viscous dissipation potential form is adopted to bring to light the incidences of the hypothesis H_1:

$$(22)\quad \phi(\dot{\beta}) = \frac{1}{2}\eta\,\dot{\beta}^2$$

4.3.1 Model 1

The free energy form, defined in part 4.1, can be decomposed into:

$$(23)\quad \rho\psi_a = \frac{1}{2}E\varepsilon^2 - \rho\frac{L}{M_s}(T - M_s) - \rho C_\alpha T\mathrm{Log}T$$

(24) $$\rho\psi_m = \frac{1}{2} E \varepsilon^2 - \rho\alpha(T)\varepsilon - \rho C_\alpha T \mathrm{Log} T,$$

where $\alpha(T)$ is defined by:

(25) $$\alpha(T) = \begin{cases} -a\,(T - M_d), & \text{if } T \leq M_d, \\ 0, & \text{otherwise}. \end{cases}$$

The symbol L is related to the latent heat; M_d is the temperature above which no transformation occurs. To obtain qualitatively realistic hysteresis loop the following coefficients have been chosen: $V_0 = 150\ mm^3$, $\rho = 7700\ Kg\ m^{-3}$, $E = 24\ GPa$, $\nu = 0.3$, $L = 1000\ J\ kg^{-1}$, $M_s = 6°C$, $M_d = M_s + 75°C$, $T_0 = 30\ °C$, $a = 147.72\ J\ kg^{-1}\ K^{-1}$, $C_\alpha = 147 J.kg^{-1}\ K^{-1}$, $\tau = 17\ s$, $|\dot{\varepsilon}| = 0.0001\ s^{-1}$.

The viscosity coefficient $\eta = 9.10^6\ J\ m^{-3}\ s$, when the transformation is dissipative.

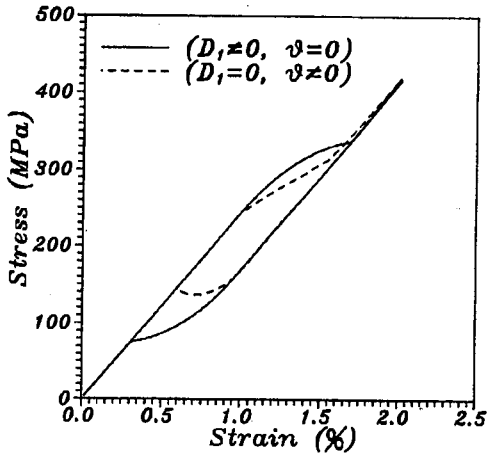

Fig.7: Mechanical responses in the case of Model 1 approach. Solid line (H_1): isothermal and dissipative process; dashed line (H_2): non-isothermal and non-dissipative process.

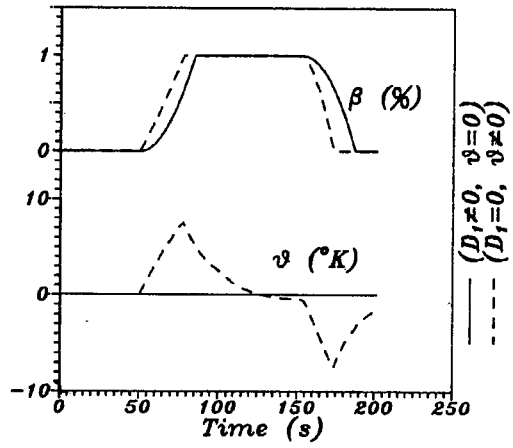

Fig.8: Evolutions of the temperature variations and kinetics of the phase change in the case of model 1. Of course, with H_1 (solid line), no temperature variation appears.

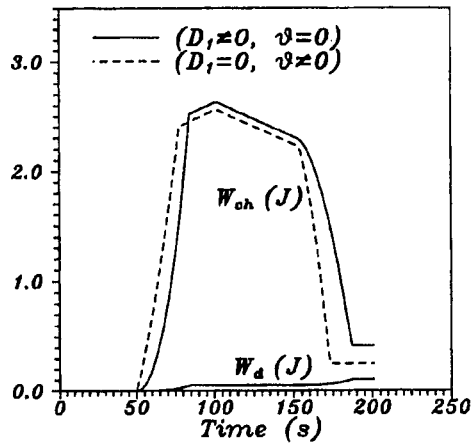

Fig.9: Energy balances (model 1). The thermo-elastic couplings are only taken into account during the phase change. The term W_d stands for the energy dissipated within the equivalent volume V_0.

4.3.2 Model 2

The different terms defined in part 4.2 can be written as:

(26) $$W_{elast} = \frac{1}{2} E(\varepsilon - g\beta)^2 - \frac{E}{(1-2\nu)} \lambda_{th} \theta \varepsilon - \rho \frac{C_\alpha}{2T_0} \theta^2$$

(27) $$W_{chem} = AT + B$$

(28) $$W_{int} = -\beta (1 - \beta) D$$

The coefficients taken in the simulations are : $V_0 = 150$ mm^3, $\rho = 7700$ kg m^{-3}, $E = 24$ GPa, $\nu = 0.3$, $\lambda_{th} = 18\ 10^{-6}$ K^{-1}, $M_s = 6$°C, $M_f = 15$°C, $T_0 = 30$ °C, $C_\alpha = 102$ J kg^{-1}.K^{-1}, $\tau = 13$ s, $|\dot{\varepsilon}| = 0.0001$ s^{-1}, $A = 45.17$ J m^{-3}K^{-1}, $B = 13028.42$ J m^{-3}, $D = 151.98$ J m^{-3}.
The viscosity coefficient $\eta = 9.10^6$ J m^{-3} s, when a dissipative process is assumed.

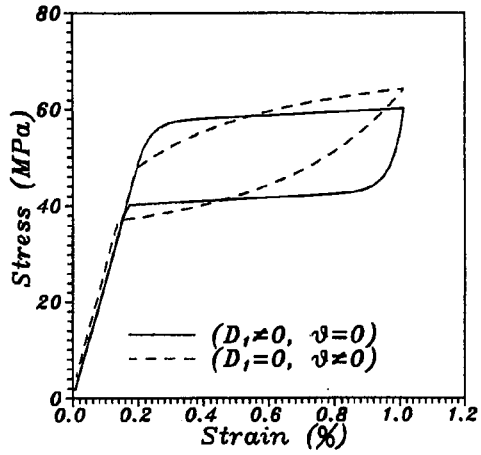

Fig.10: Mechanical responses in the case of Model 2 approach. Solid line (H_1): isothermal and dissipative process; dashed line (H_2): non-isothermal and non-dissipative process.

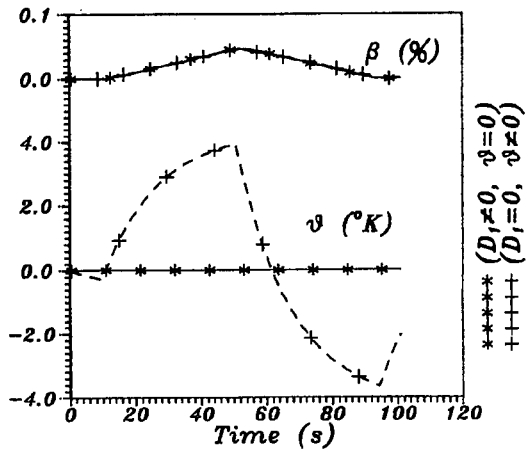

Fig.11: Evolutions of the temperature variations and kinetics of the phase change in the case of model 2.

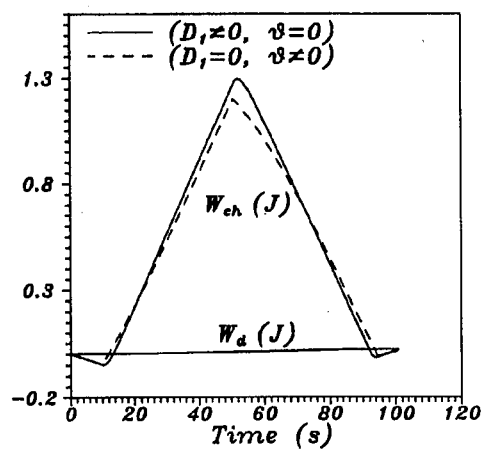

Fig.12: Energy balances (model 2).

4.3.3 Numerical results

On the figures 7 and 10, the mechanical responses for a load-unload cycle are plotted; the solid lines are used in the case of H_1, and dashed lines in the case of H_2. The variations of the temperature and the kinematics of phase change are given on figures 8 and 11. At least, the evolutions of W_{ch} and W_d can be observed on the figures 9 and 12. The term W_d is the energy dissipated within the gauge volume V_0 during the tensile test.

First, one can observe with both models that both hypotheses give an hysteresis loop of the same order of magnitude. The ratios of R_M are indicated in table 2. Second, note that even in the dissipative case (H_1), the ratio R_T is able to remain small. It comes from the set of coefficients that have been chosen to predict a small dissipation in comparison with the latent heat rate.

Tab. 2: Numerical simulation of the ratios R_T and R_M

Model (M) Hypothesis (H)	$V_0 \int_C \lvert w'_{ch} \rvert \, dt$ (10^{-3} J)	R_T (%)	$V_0 \int_C \sigma \dot{\varepsilon} \, dt$ (10^{-3} J)	R_M (%)
M_1 - H_1	4863	8,4	104	10
M_1 - H_2	4484	5,1	72	11
M_2 - H_1	2758	1	20	25
M_2 - H_2	2552	1	15	19

5. CONCLUDING COMMENTS

The austenite-martensite phase change under stress, at constant room temperature, has been studied on Cu-Zn-Al samples from a thermomechanical viewpoint. The infrared data corresponding to temperature variations of the material show that the transformations are non-isothermal processes. These variations are small (around several Celsius degrees) in comparison with the absolute temperature; but, they cannot be neglected compared to the transition domain size (around ten Celsius degrees). In a first order approximation, associating a thermodynamic cycle to each hysteresis loop yields a non dissipative process. These results justify a non-isothermal and non-dissipative process hypothesis (H_2). The incidence of such an hypothesis has been underlined using two classical models. These models have been originally developped assuming a dissipative and isothermal phase change (H_1). The performed numerical simulations show that realistic hysteresis loops can be obtained using indifferently both hypotheses H_1 and H_2.

REFERENCES

Boccara, N. 1968. Les principes de la Thermodynamique Classique. P. U. F., Coll. Sup.

Chrysochoos, A. & Dupré, J.C. in press. An infra-red set-up for Continuum Thermomechanics. Actes du colloque Q.I.R.T., July 7-9 1992, Eurotherm. Seminar 27, Editions Européennes Thermiques et Industries.

Frémond, M. 1987. Matériaux à mémoire de forme. C. R. Acad. Sci., Série 2, n°7: 239-245.

Germain, P. 1973. Cours de Mécanique des Milieux Continus, t. 1. Masson Ed.

Halphen, B. & Nguyen, Q. S. 1975. Sur les matériaux standard généralisés. J. de Méca. vol. n°14, n°1.
Lexcellent, C. & Licht, C. 1991. Some remarks on the modelling of the thermomechanical behaviour of shape memory alloys. J. de Ph. Appl., 4, C4, vol. n°1, Nov.: 35-39.
Müller, I. & Xu, H. 1991. On the pseudoelastic hysteresis. Acta. Metall. Mater., vol.39, n°3: 263-271.
Ortin, J. & Planes, A. 1988. Thermodynamic analysis of thermal measurements in thermoelastic martensitic transformations. Acta. Meta. 36, n°8: 1873-1889.
Patoor, E. & Eberhart, A. & Berveiller, M. 1987. Acta Metá. 38: 2779-2789.
Vacher, P. 1991. Etude du comportement pseudo-élastique d'alliages à mémoire de forme Cu-Zn-Al polycristallins. Thesis. Besançon, France.
Van Humbeek, J. & Delay, L. 1981. The influence of strain-rate, amplitude an temperature of a pseudoelastique Cu-Zn-Al single cristal. J. de Phys., C5, n°10, t.42: 1007-1011.